Int J Adv Manuf Technol (2017) 92:4399–4413
DOI 10.1007/s00170-017-0496-6

ORIGINAL ARTICLE

High cycle fatigue prediction of glass fiber-reinforced epoxy composites: reliability study

R. Ben Sghaier [1,2] · N. Majed [2] · H. Ben Dali [2] · R. Fathallah [2]

Received: 10 February 2017 / Accepted: 1 May 2017 / Published online: 18 May 2017

Abstract The aim of this paper is to develop a probabilistic approach of high cycle fatigue (HCF) prediction of glass fiber-reinforced epoxy composites by taking into account the modifications induced by the variation of the loading parameters (stress and number of cycles) and those of the material parameters (fiber Young's modulus and fiber volume fraction). Using fatigue curve analytical expression and Monte Carlo simulation assessment, probabilistic Wöhler curves are plotted to predict the high cycle fatigue behavior of the material. In this regard, four cases are studied by varying the hypothesis for the stress and number of cycle values to be probabilistic or deterministic. The design of experiment (DoE) techniques are used in this work by varying the factors of interest in a full factorial design to evaluate the effect and the interaction of some factors influencing the fatigue reliability. The controlled input factors of the process are traduced by (i) the materials' parameters represented by the variation of fiber and matrix Young's moduli (E_f and E_m) and the fiber volume fraction (V_f) and either traduced by (ii) the loading parameters represented by the applied stress and number of cycles.

Keywords Fatigue reliability · Glass fiber · Monte Carlo simulation · Wöhler curve · Design of experiments

✉ R. Ben Sghaier
rabibensghaier@gmail.com

[1] Higher Institute of Applied Sciences and Technology of Sousse (ISSATS) Cité Taffala (Ibn Khaldoun), University of Sousse, 4003 Sousse, Tunisia

[2] Laboratory of Mechanics of Sousse (LMS) National Engineering School of Sousse, University of Sousse, BP 264 Erriadh, 4023 Sousse, Tunisia

Nomenclature

τ_u	Ultimate shear strength
$\tau_{\max}$	Maximum shear stress
$\sigma_{\min}$	Minimum tensile stress
$\sigma_{\max}$	Maximum tensile stress
σ_u	Maximum flexural strength
E_c	Composite Young's modulus
E_{m}	Matrix Young's modulus
E_f	Fiber Young's modulus
I	Section property of the specimen
I_2	Second moment of inertia of the specimen
L	Specimen length
$G(x_i)$; $S(x_i)$; $L(x_i)$	Performance, strength, and load functions, respectively
Cv	Coefficient of variation (quotient of standard deviation and mean value)
X	Random variables
N	Monte Carlo simulation sample size of the pair (a,b)
$\frac{l}{r}$	Span-to-depth ratio
P	Applied stress
P_f	Probability of failure
R	Reliability
R_σ	Fatigue load ratio
r	Specimen radius
$\{X\}$	Vector of random variables
x_i	Element of the vector {X}
V_f	Fiber volume fraction
u	Deflection during flexural test
sa ; sb	Standard deviation of a and b Wöhler parameters
$s\sigma$	Standard deviation of the applied stress

a_0 ; b_0	Mean values of a and b Wöhler parameters
cva ; cvb	Coefficient of variation of Wöhler parameters a and b, respectively
$cv\sigma_{app}$; cvN_{cyc}	Coefficient of variation of the applied stress and of the number of cycles, respectively
i	Computing index for (a,b) random sampling
j	Computing index of the stress beam lines
k	Computing index of the loading random sampling
N_{tot}	Random sampling size

1 Introduction

Over the past few decades, the use of composite materials for various structural applications has received wide acceptance. Several reasons have been advanced to justify the popularity of composite materials: high strength-to-weight ratios in comparison with many other materials, advances in processing, high-volume production, and structural performance. Besides, composite materials give unique opportunities in the area of new structural materials, since the choice of reinforcements and matrices offers a large variety of composites.

Composites reinforced with glass, carbon, Kevlar, or even natural fibers are well-known for their good fatigue behavior, especially when loading is applied in the direction of the reinforcement [1, 2]. These composites find extensive use in applications where structures are cyclically loaded with relatively low stress values such as automotive, electronics, housing construction, furniture, sports goods, and many others. The fatigue behavior, even under this simple loading condition, is complex and difficult to describe quantitatively.

To predict high cycle fatigue (HCF) behavior of composites, many research works have been undertaken; a review of the literature on related researches has been presented by Degriek et al. [3] and Wicaksono et al. [4]. There are currently three main groups of composite fatigue approaches: fatigue life and phenomenological and progressive damage models.

The fatigue damage has been studied in many works basing on the analysis of the evolution of residual strength [5, 6] and residual stiffness [7]. Other works discussed the fatigue life prediction basing on the analysis of the progressive damage growth or the residual properties [8–11].

Progressive damage and phenomenological approaches are very complex and expensive in terms of computational solution as well as in terms of the number of experiments needed to fully characterize the material properties. The fatigue life approach is rather straightforward and simple from the computational and experimental point of view [12, 13]. Recent studies have the advantage to use numerical simulation by finite element analysis [14]. Current fatigue life models normally utilize one of the failure criteria as the base and an empirical S–N curve as an input [15, 16]. Such fatigue life models can be used to predict the number of cycles to failure under fixed loading conditions, without taking into account damage accumulation [3, 17–19].

For the majority of cases, the approaches mentioned above remain deterministic. However, a second probabilistic category of models includes the uncertainties to predict the fatigue life of composite materials [20–25]. Considering the development of the reliability fatigue-based methods taking into account the scatterings and the significant dispersions related to the used geometrical and material parameters [26, 27], it seems to be necessary and with substantial benefit to analyze the HCF behavior of composites using probabilistic methods. Indeed, these stochastic approaches used for the assessment of fatigue reliability have attracted significant attention in the recent studies [28–32]. Consequently, the fatigue reliability computation becomes more and more considered as an engineering design way, which takes into account the various uncertainties corresponding to the different fatigue parameters.

In the present work, a probabilistic prediction of the HCF behavior of glass fiber-reinforced epoxy composites is developed. It is based on the *S-N* (Wöhler) curve analytical expression and the Monte Carlo simulation assessment. By taking into account the variation of the composite material parameters (a,b) and the loading parameters (σ,N), probabilistic *S-N* Wöhler curves are plotted to predict the high cycle fatigue life. Two different cases are discussed and compared: the first is fibers provided from several suppliers and the second is fibers provided from only one supplier. The DoE techniques are used in this work by varying the factors of interest in a full factorial design to assess the effect and the interaction of some factors influencing the fatigue reliability.

2 Background

2.1 *S-N* curve

Fatigue is defined as "the weakening of a material caused by repeatedly applied loads." It is the progressive and localized structural damage that occurs when a material is subjected to cyclic loading.

The fatigue test parameters are the minimum/maximum stress ratio R_σ ($R_\sigma = \frac{\sigma_{\min}}{\sigma_{\max}}$), the frequency, and the maximum stress.

To analyze the results, the most well-known endurance diagram is the *S-N* curve (stress–number of cycles) or Wöhler curve: it displays the imposed stress levels (e.g., the

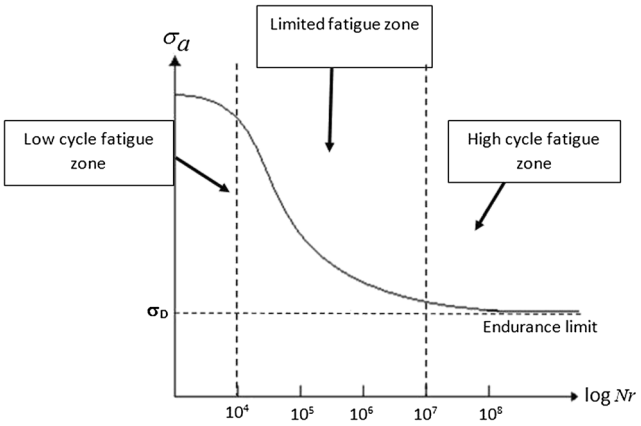

Fig. 1 Wöhler curve and fatigue zone classification

maximum stress) against the number of cycles to failure N_r (generally a logarithmic scale). A large number of tests must be conducted during the fatigue test campaigns since the results are generally highly dispersed. For a given level of stress, therefore, the N_r may extend over a decade, a situation which is partly due to the experimental conditions but more especially to the phenomena involved in crack initiation and propagation. Figure 1 shows an example of *S-N* curve and indicates the three fatigue regions:

- Low cycle fatigue: Under high stresses generating plastic strains and small numbers of cycles to failure (often from just a few cycles up to 10^4 cycles)
- High cycle fatigue: Failure still occurs, but the lifetime increases when the stress level decreases
- Fatigue limit, under which fatigue failure no longer occurs, is frequently observed: In this case, the *S-N* curve extends towards a horizontal asymptote (this region often concerns the number of cycles to failure $N_r > 10^7$ or 10^8). This asymptote is not always the rule, however, especially when other damage such as corrosion occurs in addition to mechanical fatigue

It is well established in fatigue studies that for HCF ($10^4 < N_r < 10^7$), a "duplex *S-N* curve" occurs [33, 34].

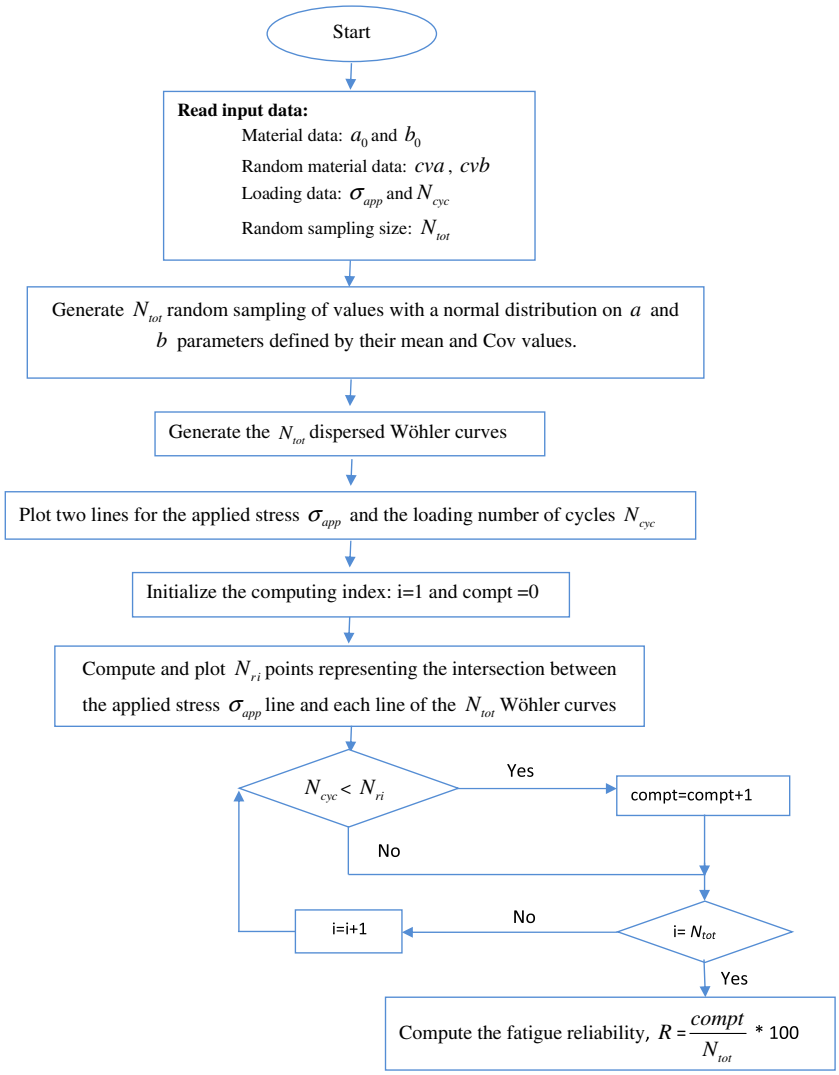

Fig. 2 Flowchart for the HCF reliability calculation (case 1)

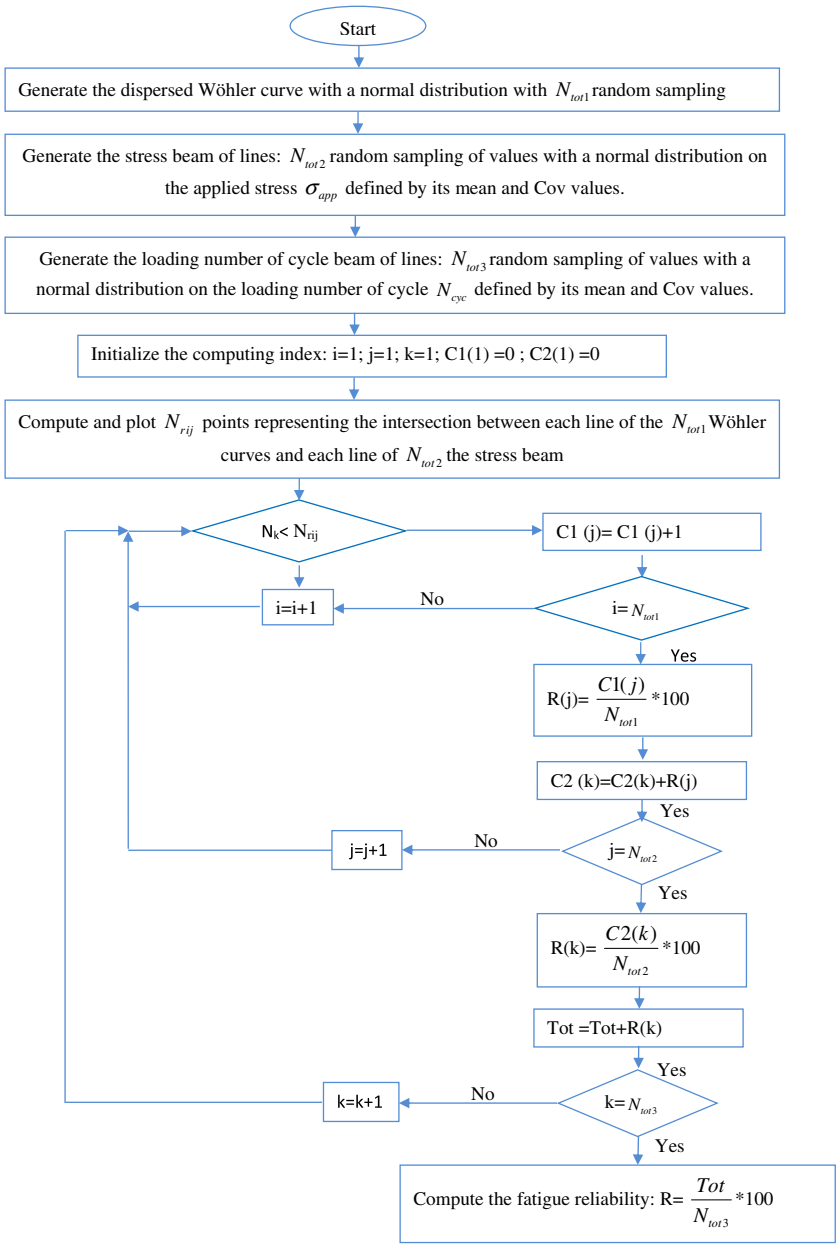

Fig. 3 Flowchart for the HCF reliability calculation for cases 2, 3, and 4

Deterministic and probabilistic approaches have been proposed to take into account this phenomenon. Numerous standards and opening procedures, especially statistical, are available to conduct the tests. Probabilistic failure curves (at 90%, 50% survival) for example can be plotted on the endurance diagram.

2.2 Probabilistic approach

To compute the reliability, one considers a vector of random variables $\{X\}$ representing uncertain structural quantities. Let x_i be an element of the random vector $\{X\}$, with a probability density function (PDF) $f_{X_i}(x_i)$. A performance function $G(\{x\})$, separating the security and the failure fields, is written as follows:

$$G(\{x\}) = S(\{x\}) - L(\{x\}) \tag{1}$$

where $G(\{x\}) = 0$ is the limit state function, $S(\{x\})$ is the strength function, and $L(\{x\})$ is the load function [35, 36]. The probability of failure P_f is given by:

$$P_f = \int_{G(\{x\})<0} f_{\{X\}}(\{x\})\, dx_1 \ldots\ldots dx_n = \Pr(L(\{x\}) > S(\{x\})) = \Pr(G(\{x\}) < 0) \tag{2}$$

In that case, if the inequality $G(\{x\}) \geq 0$ is satisfied, this indicates a structural safety condition. In the opposite

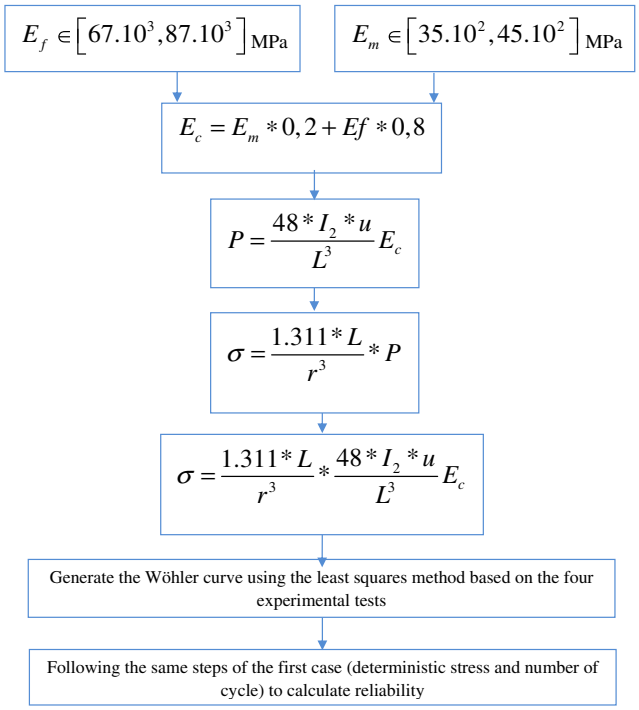

Fig. 4 Calculation flowchart to study the influence of Young's modulus

case, if $G(\{x\}) < 0$, this means a structural failure condition.

To compute the probability of failure P_f, Eq. 2, one can use many approaches such as analytical resolution, approximate computational methods, and the Monte Carlo simulation [35, 36].

In this work, the last approach has been used. In fact, when the performance function is defined over a vector of more than two random variables, the joint probability density function of X is practically difficult to find. The Monte Carlo simulation method remains often the only means of taking into account certain nonlinear behavior. Such procedure is simple; however, it has the drawback to have a large number of runs possibly required to obtain an accurate result. Its convergence speed is low and it is proportional to $\sqrt{N}$ [37].

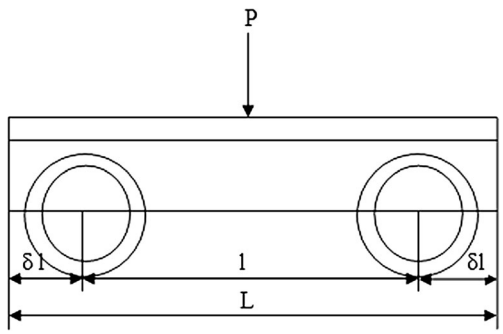

Fig. 5 Three-point flexural test for a semi-circular specimen [39]

Table 1 Geometrical properties of the semi-circular specimen [39]

r (mm)	$\frac{l}{r}$	L (mm)
6.5	16	$=l + 2 \times \delta l = l + 2 \times 10\% l = 120 \times \% l$

Let $I(\{x\})$ denotes an indicator failure function where:

$$I(\{x\}) < 0 = \begin{cases} 1 & \text{if } G(\{x\}) < 0 \\ 0 & \text{if } G(\{x\}) \geq 0 \end{cases} \quad (3)$$

$$P_f = \int_{D_f} I(\{x\}) f_{\{X\}}(\{x\})\, dx_1 \ldots\ldots dx_n \quad (4)$$

where D_f denotes the failure space defined by $G(\{x\}) < 0$. By introducing $I(x_i)$in Eq. 4, $P_f$becomes the expectation value of $I(x_i)$:$E[I(x_i)]$.

Using several random samplings, the Monte Carlo method aims to simulate a high number of load and strength values according to their PDF. Let N be the total number of simulation events. For the N computed values of $G(\{x\})$, it is assumed that the failure event frequency, where $G(\{x\}) < 0$, extends towards the failure probability P_f when $N \rightarrow +\infty$ [36].

$$P_f = \lim_{N \rightarrow +\infty} \frac{\text{Number of failure events } G(\{x\}) < 0}{\mathrm{N}} = \lim_{N \rightarrow +\infty} \frac{1}{N} \sum_{i=1}^{N} \mathrm{I}(\{x\}) \quad (5)$$

For a given coefficient of variation of P_f equal to 0.1 and for $P_f = 10^{-n_0}$, the number of Monte Carlo simulations needed $\mathrm{N} = 10^{n_0+2}$ (i.e., $P_f = 0.01, N = 10^4$) [35, 38]. In this paper, N is taken equal to 10^4. It is an acceptable computational cost especially in the case of explicit function.

The reliability R is given by the following relationship:

$$R = 1 - P_f \quad (6)$$

3 HCF reliability calculation

3.1 Wöhler curve analytical expression

Many analytical expressions have been proposed to plot the Wöhler curve for the limited and unlimited endurance zones. The model used in this work is the Wöhler law:

$$\sigma_a = \mathrm{b} - \mathrm{a} \cdot \log \mathrm{N_r} \quad \mathrm{a} > 0; \mathrm{b} > 0 \quad (7)$$

with σ_a alternate stress amplitude and N_r number of cycles to failure.

In this work, we attempt to study the practicability of the probabilistic approach, by taking into account the variation of the composite material parameters (a,b) and the loading

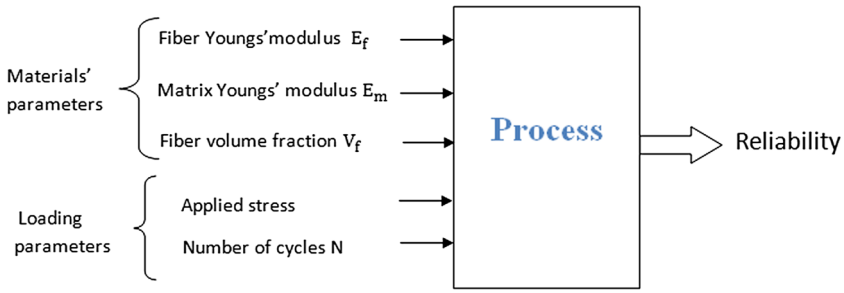

Fig. 6 Inputs/outputs of DoE

parameters (σ_{app}, N_{cyc}). These parameters with their dispersion are integrated into the probabilistic model to predict the high cycle fatigue behavior of the material.

3.2 Calculation steps

We suppose that a and b are two random variables defined by their mean values a_0 and b_0 and their coefficient of variation (cva) and (cvb). By making a random sampling using the Monte Carlo method, we obtain a straight line for each (a,b) pair, which results in a beam lines leading to three zones: (i) a failure zone, (ii) a resistance zone, and (iii) an uncertain zone. For each point defined by stress amplitude and number of cycles, we can determine the reliability value. The flowchart of Fig. 2 represents the fatigue reliability calculation steps in the case of deterministic values of stress and number of cycles (case 1). When one or more of these values are probabilistic (cases 2, 3, and 4), the calculation steps are developed in the flowchart of Fig. 3 to evaluate the fatigue reliability.

3.3 Parameters influencing the fatigue behavior of composites

The fatigue behavior of fiberglass composites can be influenced by many factors such as type of fiber, fiber mechanical properties, fiber strength and modulus, fiber-matrix adhesion, environmental temperature, etc. In this work, we focus our study on the influence of glass fiber and matrix Young's modulus and the fiber volume fraction.

A computing code was developed under MATLAB® software to study the influence of Young's modulus variation on the Wöhler curve for the flexural test. The calculation steps are represented in flowchart of Fig. 4.

The approach for the reliability calculation is described as follows: Four experimental test points have been taken from the flexural-fatigue curve, which represents the standard stress (ratio of applied and ultimate stresses) versus the number of cycles to failure [39]. The four taken points coordinates are respectively [(1,100%); (20, 80%); (10^2, 70%); and (10^3, 60%)].

For σ_u = 1660 MPa [39], the four-point coordinates in S-N diagram are then [(1, 1660); (20, 1328); (10^2, 1162); and (10^3, 996)].

We have:

$$\sigma = \frac{1.311 \times L}{r^3} \times P \tag{8}$$

with P applied stress, l span length, L specimen length, δl cantilever length represents 10% of the span length, and $I_2 I_2$ second moment of the specimen area (Fig. 5).

From Table 1, we obtain l = 104 mm and L = 124.8 mm. By introducing these geometrical values in (Eq. 8), we can deduce the following relationship between load and stress:

$$P_i = \frac{\sigma_i}{0.6} \tag{9}$$

Consequently, the loading values corresponding to the four studied points are as follows:

$$P_i\,(N) = [2766,66; 2213,33; 1936,66; 1660]$$

Table 2 Materials and loading parameters values at different levels

Factor	Variation of E_f (MPa)	Variation of E_m (MPa)	Variation of V_f (%)	Stress (MPa)	Number of cycle exponent factor $N(10^N)$
Level (−1)	1000	100	10	1000	7
Minimum value Level (0)	10,500	550	30	1400	8.5
Mean value Level (1)	20,000	1000	50	1800	10
Maximum value					

Table 3 Material properties used during Adimi tests [39]

T (°C)	Ultimate shear strength (MPa)	Slope of the curve $^{\tau_{max}}/_{\tau_u}$	Endurance limit (MPa)
Room temperature (20)	83.20	−3.69	42
100	64.40	−4.21	25

From the force deflection curve [39], we can find the displacement (mm) during the flexural test corresponding to an applied stress (N) for a span-to-depth ratio $\frac{l}{r} = 16$.

The displacement values corresponding to the four studied points are as follows:

$$u_i\ (\text{mm}) = [\,6.5; 5.2; 4.6; 3.8\,]$$

By using the Bazergui formula for a three-point bending flexural test, we can plot the stress which depends on the probabilistic Youngs' modulus as a function of the number of cycles to failure.

$$P = \frac{48 \times I_2 \times u}{L^3} \times E_c \tag{10}$$

$$I_2 = 0.11 \times r^4 \tag{11}$$

From Eqs. 10 and 11, we deduce:

$$P = 2.88 \cdot 10^{-3} \times u \times E_c \tag{12}$$

The Young's modulus of the composite used is expressed by the following formula:

$$E_c = E_m \times 0.2 + E_f \times 0.8 \tag{13}$$

For glass fibers, Young's modulus ranging between $[67 \cdot 10^3]$ and $[87 \cdot 10^3]$ (MPa) and epoxy Young's modulus ranging between $[35 \cdot 10^2]$ and $[45 \cdot 10^2]$ (MPa), the equivalent composite Young's modulus E_c and, therefore, the applied stress P dispersion can be described each one by a vector of random values representing their probabilistic distribution.

The four points are inserted into a computation code under Matlab®, and using the least squares method, a probabilistic Wöhler curve is obtained.

3.4 Wöhler curve plotting

For this case, the Wöhler curve can be plotted using the least squares method. By using Eq. 7 and taking into consideration the experimental error, the Wöhler equation becomes:

Table 4 Elastic material properties [39]

Elastic properties	
Shear modulus (GPa)	Flexural modulus (GPa)
5.39	54

Table 5 Material properties used to obtain Fig. 13

E_f (MPa)	E_m (MPa)	V_f (%)	Stress (MPa)	Number of cycles
[76,500 87,000]	[4400 4500]	[75% 80%]	1400	10^{10}

$$y = \mathrm{Ax} + \mathrm{B} + \mathrm{e} \tag{14}$$

With $B = a$; $A = -b$; $Y = \sigma_a$; $X = \log N_r$

With $e_i = y_i - (Ax_i + B)$, where e_i is the difference between the regression line and the considered point.

The quadratic error summation function is expressed as follows:

$$Q(A,B) = \sum_{i=0}^{n} {e_i}^2 = \sum_{i=0}^{n} \left(y_i - (Ax_i + B)\right)^2 \tag{15}$$

In order to find the minimum of this function and by using the least squares method, we find:

$$A = \frac{\sum_{i=0}^{n} x_i y_i - (n+1)\overline{x} \cdot \overline{y}}{(n+1)Vx} \tag{16}$$

$$B = \frac{\sum_{i=0}^{n} y_i - A \sum_{i=0}^{n} x_i}{(n+1)} \tag{17}$$

For Wöhler equation, the identified parameters are:

$$B = a; A = -b; y = \log\sigma_a; y = \log\sigma_a; x = \log N_r.$$

Consequently, both a and b parameters are determined.

4 Factors influencing assessment

The DoE techniques are used in this work by varying the factors of interest in a full factorial design to assess the effect and the interaction of some factors influencing the fatigue reliability. The goal is always to allow the experimenter to evaluate in an unbiased (or least biased) way the consequences of changing the settings of a particular factor, that is, regardless of how other factors were set. This would work fine, except that the number of necessary runs in the experiment observations (or numerical calculations) is very important. However, this formulation shows how important factors affect the response and leads to the development of first- and second-order polynomial models that include the parameters under consideration and their statistical significance. This method uses

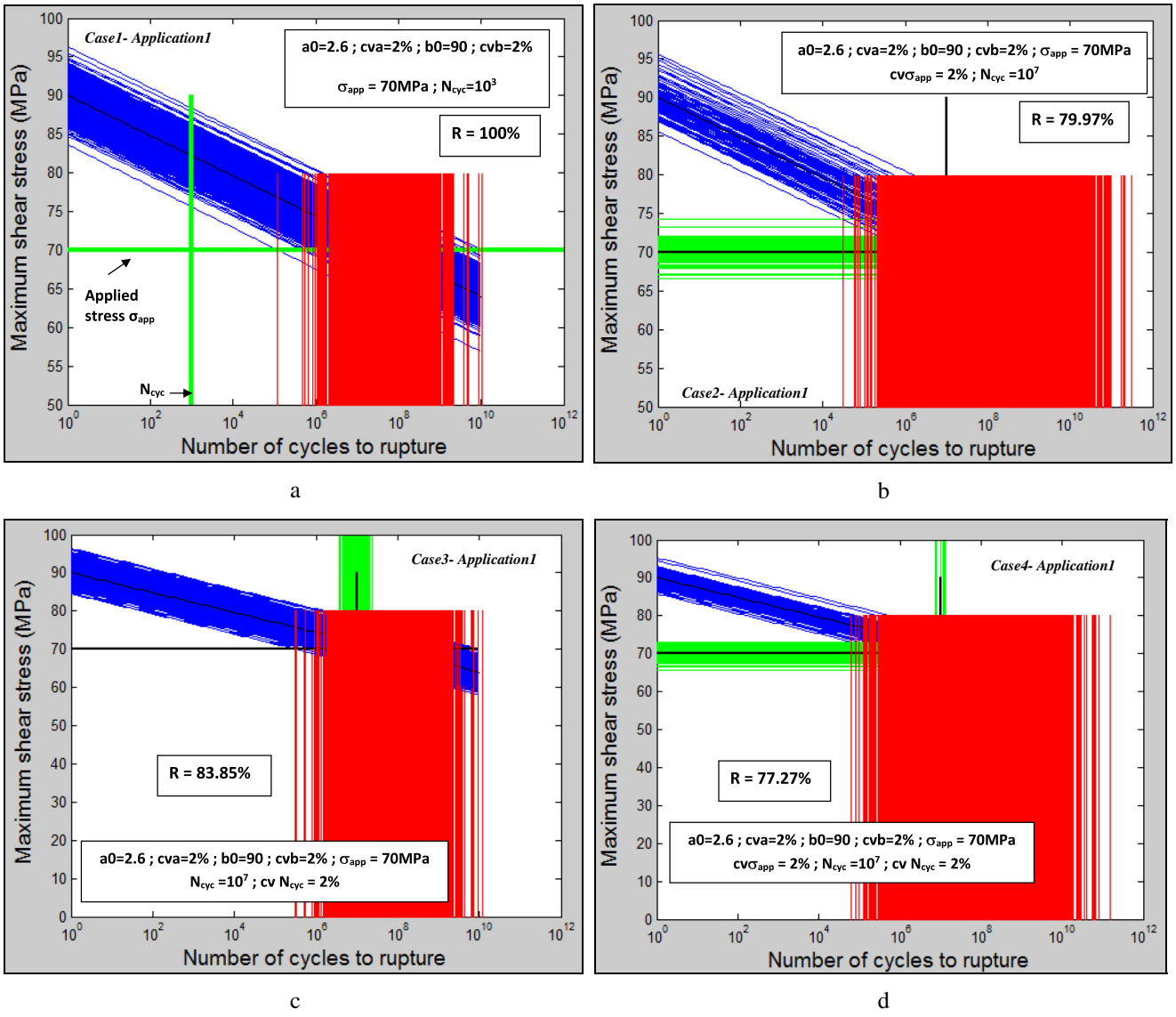

Fig. 7 Probabilistic Wöhler curve for **a** deterministic stress and number of cycles, **b** probabilistic stress and deterministic number of cycles, **c** deterministic stress and probabilistic number of cycles, and **d** both probabilistic stress and number of cycles

statistical tools such as response graph and analysis of variance (ANOVA) techniques which are used and developed under *Minitab® V14* software.

This approach is planned in the following scheme of investigation:

1. Identifying the important factors which have influence on the fatigue life
2. Finding the scatter range of each factor characterized by their coefficient of variation
3. Developing the numerical design matrix
4. Conducting the numerical calculations according the planned design matrix
5. Developing the mathematical models (if required)
6. Calculating the coefficient of the factors and their interactions: For the convenience of recording and processing experimental or numerical data, highest and lowest and middle levels of factors have been coded as +1 and −1 and 0, respectively, and the coded values $i\,z$ of any intermediate levels can be

The controlled inputs factors of the process are classified as follows (Fig. 6):

1. The materials' parameters represented by the variation of fiber and matrix Young's moduli (E_f and E_m) and the fiber volume fraction (V_f)
2. Loading parameters represented by the applied stress and number of cycles

The levels of the inputs values are presented in Table 2.

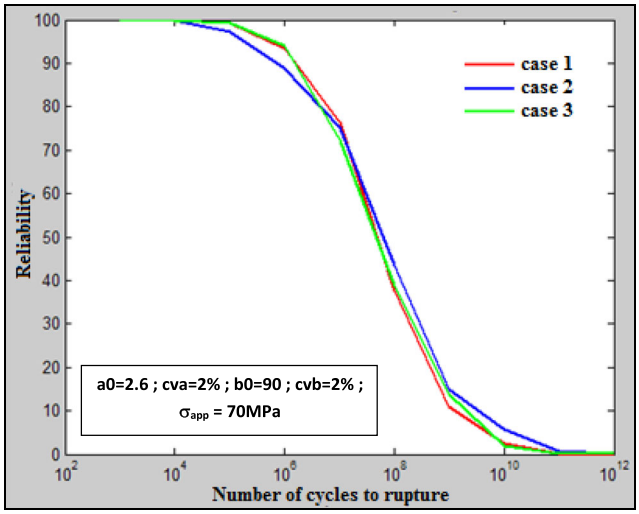

Fig. 8 Variation of the reliability with the number of cycles for the three first cases

5 Applications

In order to validate the proposed approach, we use in this work available results of exhaustive experimental investigations

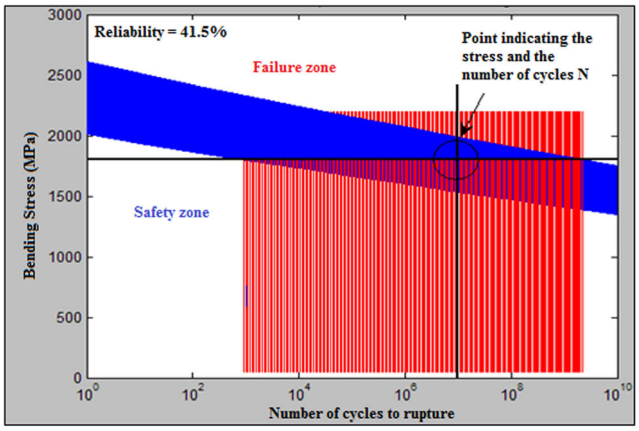

a

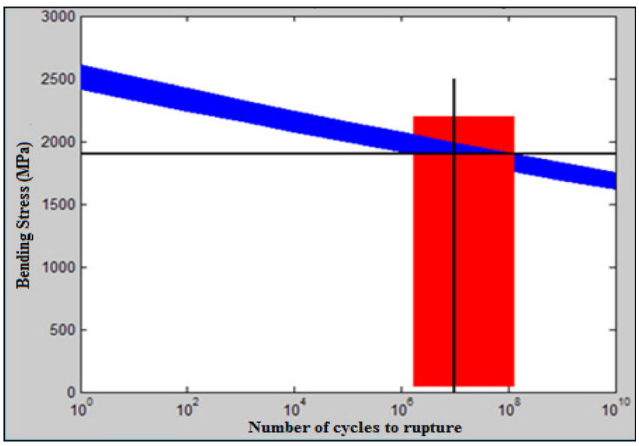

b

Fig. 9 Probabilistic Wöhler curve for the flexural-fatigue test. **a** Fibers provided from many suppliers. **b** Fibers provided from one supplier

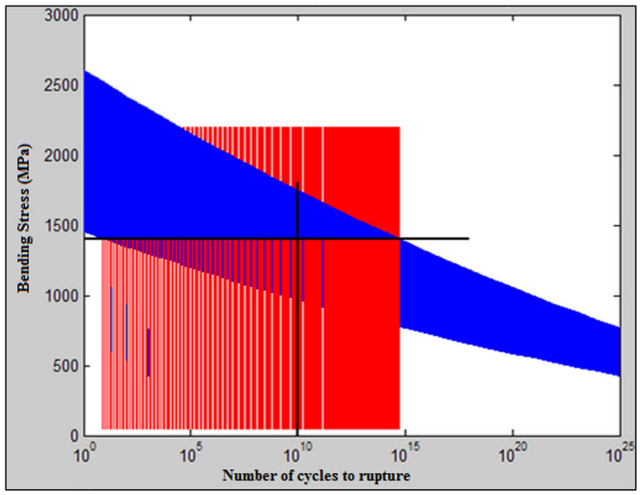

a

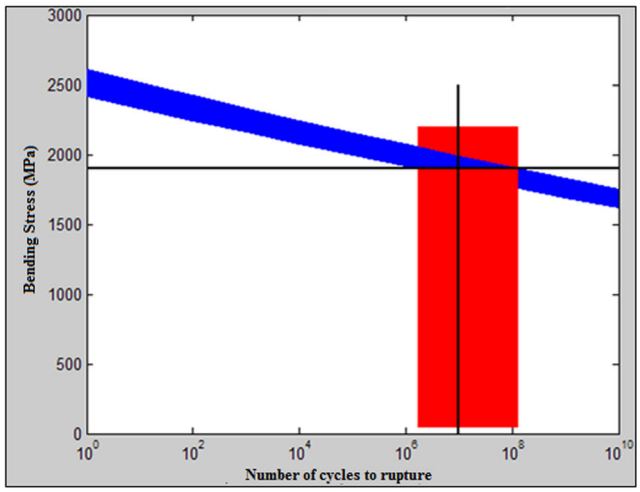

b

Fig. 10 Probabilistic Wöhler curve for the flexural-fatigue test—Young's modulus and fiber volume fraction dispersion. **a** Fibers provided from many suppliers. **b** Fibers provided from one supplier

carried out by Adimi [39–41]: fiber glass-reinforced epoxy composites with semi-circular-shaped specimen manufactured by the pultrusion process. The radius is on the order of 6.5 mm and the length of 400 mm. The fiber volume fraction is chosen between 30 and 80%. The mechanical and elastic properties of this material are shown in Tables 3, 4 and 5.

6 Results and discussion

6.1 HCF reliability calculation

1. *First case: deterministic stress and number of cycles*

For a case defined by deterministic values of applied stress σ_{app} and test duration (loading number of cycle) N_{cyc}, as

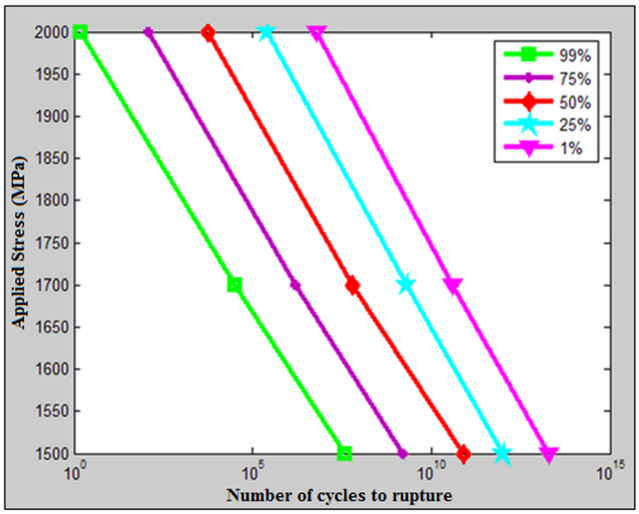

a

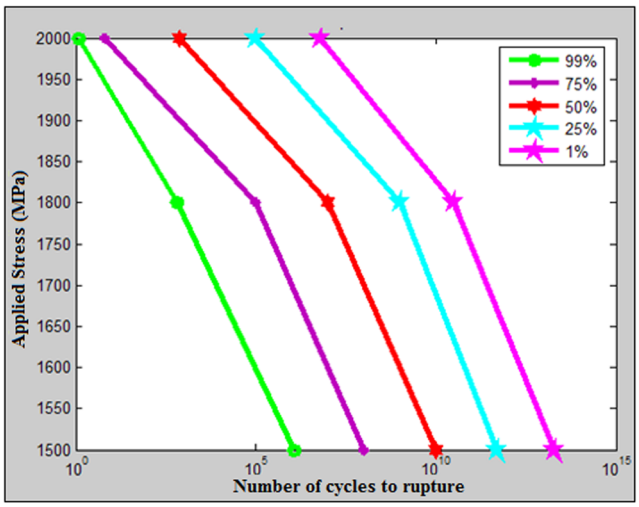

b

Fig. 11 Iso-probabilistic Wöhler curves (fibers provided from many supplier). **a** Young's modulus dispersion. **b** Young's modulus and fiber fraction dispersion

shown in Fig. 7a, the intersection between the stress line and the dispersed Wöhler curve (blue-colored) gives the red-colored points defined by N_{ri}. Fatigue reliability R is evaluated as follows:

$$R = \frac{\text{number}\left(N_{cyc} < N_{ri}\right)}{N_{tot}} \tag{18}$$

We notice that N_{ri} values are within the range of $[10^5, 10^6]$. For the defined stress value, if the number of cycles N_{cyc} is less than 10^5, the reliability is then equal to 100%. Otherwise, if the number of cycles is more than 10^6, the reliability is 0%. If the number of cycles N_{cyc} is belonging to the interval of $[10^5, 10^6]$, the reliability can vary between 100 and 0%.

2. *Second case: probabilistic stress and deterministic number of cycles*

For a probabilistic value of stress σ, the green beam lines in Fig. 7b show the normal distribution of σ defined by the mean and Cov values. The value of the test duration N remains deterministic (one line). In this case, the intersection between each line of the N_{tot1} Wöhler curves and each line of N_{tot2} stress beam lines gives the red-colored $N_{r(i,j)}$ points. Fatigue reliability $R$is evaluated as follows:

$$R = \frac{1}{N_{tot2}} \sum_j \left(\frac{\text{number}\left(N_{cyc} < N_{rij}\right)}{N_{tot1}} \right) \tag{19}$$

N_{tot1} in this case is the sample size of Wöhler curves, and N_{tot2} is the size on the random sampling on the stress beam of lines.

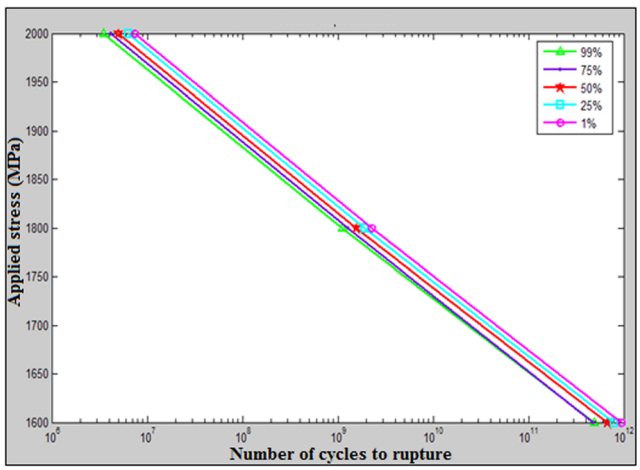

a

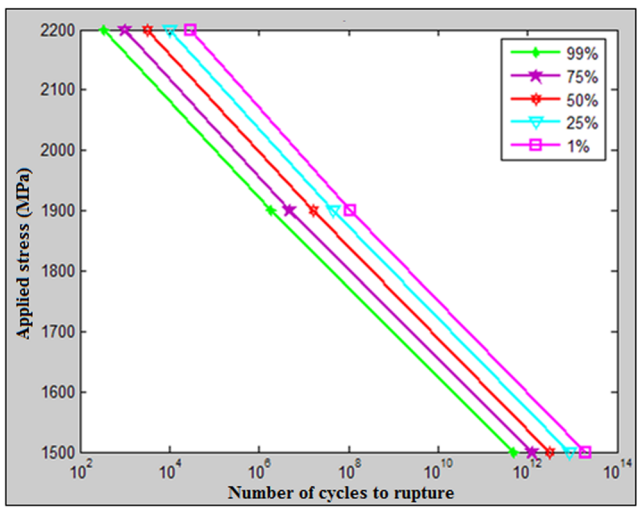

b

Fig. 12 Iso-probabilistic curves (fibers provided from one supplier). **a** Young's modulus dispersion. **b** Young's modulus and fiber fraction dispersion

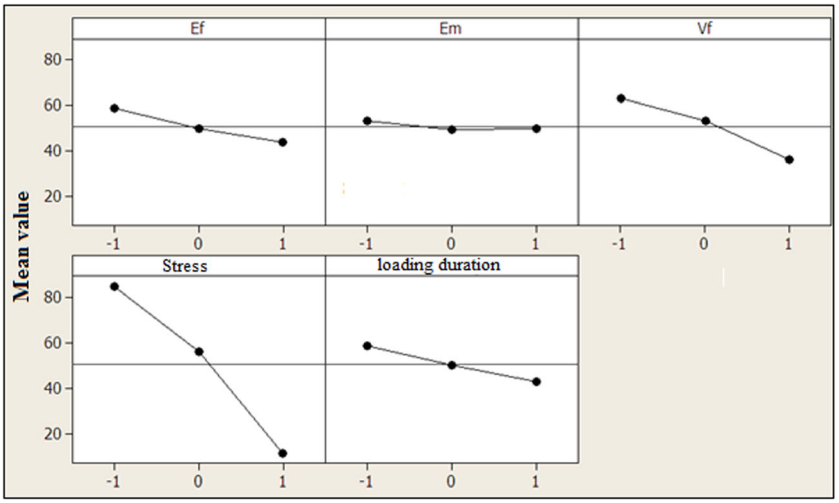

a

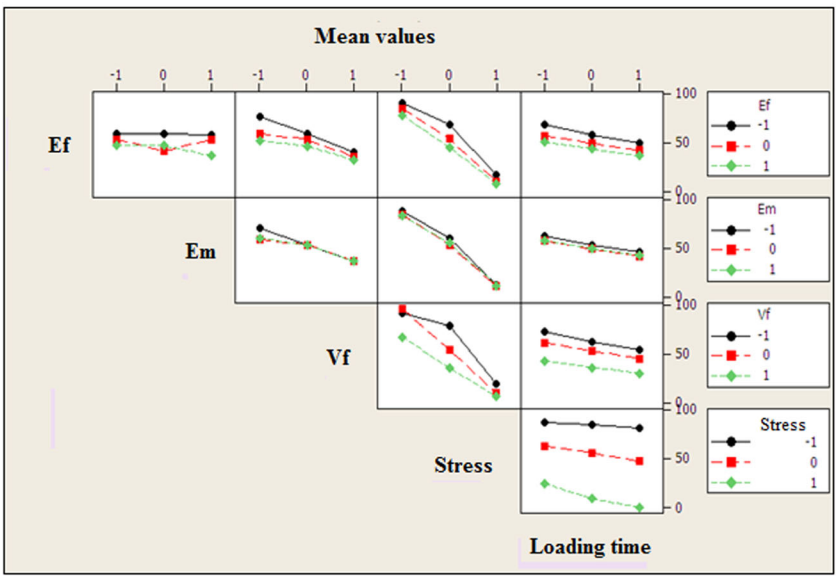

b

Fig. 13 Analysis of effects. **a** Diagram of main effects on reliability. **b** Diagram of interactions

3. *Third case: deterministic stress and probabilistic number of cycles*

By taking the same calculation steps of the last case, we reverse the characteristics of N and σ values. Thus, we generate N_{tot2} random sampling of values with a normal distribution on the loading test duration defined by its mean and Cov values, and we replace: $N < N_{r(i,j)}$ by $N_j < N_{ri}$.

The fatigue reliability R is then calculated as follows:

$$R = \frac{1}{N_{tot2}} \sum_j \left(\frac{\text{number}\left(N_j < N_{ri}\right)}{N_{tot1}} \right) \tag{20}$$

N_{tot1} remains the sample size of Wöhler curves, and N_{tot2} defines in this case the size on the random sampling on loading number of cycles (Fig. 7c).

4. *Fourth case: both probabilistic stress and number of cycles*

For this case, both stress and loading duration are probabilistic according to a normal distribution law defined by mean and Cov values. The applied stress sampling is represented by green horizontal lines in Fig. 7d and the loading by green vertical lines. Both second and third cases are combined. For each case from the N_{tot3} number of cycle random sampling, the intersection between each line from the N_{tot2} stress beam of lines and the N_{tot1} dispersed Wöhler curve (blue-colored) gives N_{rij} points. Fatigue reliability R is expressed in this case as follows:

$$R = \frac{1}{N_{tot3}} \sum_k \left(\frac{1}{N_{tot2}} \sum_j \left(\frac{\text{number}\left(N_{cyc} < N_{rij}\right)}{N_{tot1}} \right) \right) \tag{21}$$

N_{tot1} is the sample size of Wöhler curves, N_{tot2} is the size on the random sampling on the stress beam of lines, and N_{tot3} is the size on the random sampling on loading number of cycles.

5. *Influence of number of cycles parameter on the reliability*

In this application, we try to study, for the three first cases of HCF reliability calculation and for the same stress value ($\sigma_{app} = 70$ MPa), the variation of the reliability versus the test duration (number of cycles to failure). We notice from Fig. 8 that, for an applied number of cycles less than 10^7, the reliability of both second and third cases is better than that of the first case. Whereas, if the applied number of cycles is more than 10^7, the reliability of the first case is better.

6.2 Parameters influencing the fatigue behavior of composites

In this section, two different cases are discussed. In the first case (Fig. 9a), we consider that the glass fibers are obtained from many different suppliers. Thus, the fibers' Young's modulus values vary within the range of [67,5 ; 87] (10^3 MPa). For loading conditions defined by (i) a stress value $\sigma$of 1800 (MPa), (ii) a loading test duration N of 10^7, and (iii) a reliability of 41.5%, if $N < 10^3$, the reliability is 100% (safety zone), whereas for $N < 10^9$, the reliability is 0% (failure zone). For $<10^3 < N < 10^9$, the reliability varies between 100 and 0%.

The second case discussed is when glass fibers are obtained from one unique supplier (Fig. 9b). In this case, we consider that glass fibers' Young's modulus vary within the range of [86 ; 87] (10^3 MPa).

In both cases defined previously, the variety of glass fibers Young's modulus induces a dispersed Wöhler curve, and by decreasing those Young's modulus values, the composite withstands less loading. This result is expected since the composite Young's modulus decreases with the decrease of fiber and matrix ones.

To study the effect of Young's modulus and fiber volume fraction parameters, we suppose that the Young's modulus values of the matrix and glass (E_m and E_f, respectively), are both dispersed, as well as the fiber volume fraction V_f.

In the case of several glass fiber suppliers, we assume that the glass fibers are purchased from many different suppliers and their Young's modulus values vary within the range of [76,5 ; 87] (10^3 MPa).

Using the material properties presented in Tables 4 and 5, we obtain the probabilistic Wöhler curve for the flexural-fatigue test shown in Fig. 10a.

For the second case (one glass fibers supplier), we suppose that glass fibers are provided from only one supplier and, as a result, their Young's modulus values vary within the range of [86,000 87,000] (MPa). Figure 10b shows the probabilistic Wöhler curve for the flexural-fatigue test.

We point out from Fig. 10 that the decrease of the fiber volume fraction induces a decrease of the applied stress and the material becomes weaker. Furthermore, the Wöhler curve becomes more dispersed. This result could be explained by the fact that the fiber volume fraction V_f and the composite Youngs' modulus E_c are proportional and related by the rule of mixture equation:

$$E_c = E_m \times \left(1 - V_f\right) + Ef \times V_f \tag{22}$$

This result seems to be physically coherent with many studies which demonstrated that the increase of glass fiber volume fraction increases the glass/epoxy composite life [42, 43].

6.3 Iso-probabilistic Wöhler curves

To plot iso-probabilistic Wöhler curves, we have used the computing code developed under Matlab® which was described previously: the approach consists on fixing a stress value for a given reliability level and then seeking for the relevant number of cycles to rupture.

For the first applications presented below, we suppose that fibers are provided from many suppliers.

Figure 11 shows that for a given value of applied stress, the reliability and the number of cycles to failure are inversely related. For instance, if the stress value is 2000 MPa (Fig. 11a), the number of cycles to rupture equals 0 for a reliability of 99% and more that 10^2 cycles for a reliability of 75% and it reaches 10^4 cycles for a reliability of 50%. Besides, by taking into consideration the dispersion of fiber volume fraction (Fig. 11b), we have to decrease the applied stress value to reach the same reliability level.

For the second case, we assume that the glass fibers are provided from one only supplier, and the Young's modulus of those fibers varies within the range of [86,000 87,000] (MPa).

Taking into consideration the material parameter dispersion (Young's modulus and fiber volume fraction), Fig. 12 shows the iso-probabilistic curves plotted for five reliability values (1, 25, 50, 75, and 99%). We notice that reliability is better for a limited number of cycles to rupture.

6.4 Analysis of effects

The analysis of the main effects of the studied input parameters E_m, E_f, and V_f, the applied stress, and the loading duration N on the output response (reliability) are presented in Fig. 13a.

We note that the factors of stress, V_f, E_f, and N, have decreasing effect on the reliability, whereas the factor E_m has a negligible effect.

1. The most significant factor on the reliability is observed for the stress variation. When this latter reaches minimum value, the reliability has a maximum value exceeding 80%, and for the highest stress value, the reliability decreases until 0%. This result may be explained by the repetitive nature of the stress, so that it induces cumulative effect influencing the reliability value.
2. The variation of V_f has a significant effect on the reliability but at a lower intensity compared to the stress variation. For a minimum variation of V_f [70% 80%], the reliability slightly exceeds 60%. If the variation of V_f is at its mean value [50%, 80%], the reliability is at the order of 50%, and for maximum variation of V_f, the reliability decreases until 35%.
3. The effect of E_f variation is slightly less significant than that of V_f variation. For minimum E_f variation [7650, 87,000] (MPa), the reliability is about 60% and it decreases until 40% for maximum E_f variation [76,000, 87,000(MPa)].
4. The loading duration also has an effect on the reliability but with a lower intensity compared to those of the previous factors. The reliability decreases from 60 to 40%, when jumping from minimum to maximum levels.
5. The variation of E_m has no considerable effect the reliability. This may be explained by the fact that the main role of the matrix is to transfer the mechanical load to fibers, and the variation of the matrix Young's modulus has no significant impact on the reliability.

For a complex system, parameters are rarely independent and the effect that a parameter has on a response depends on the value of other parameters. For this case, in addition to the main effects, it is important to check for interaction effects. Figure 13b shows the effect of interactions between the studied parameters on the reliability response.

An interaction between two parameters is considered as negligible when the effect of the first parameter on the response is not affected by the level of the second parameter. This is represented by two parallel lines on the interaction plot. Figure 13b shows that all the interactions with the stress variation induce a significant effect. The interactions with V_f and E_f variations have less significant effects.

7 Conclusion

In this work, a probabilistic prediction of the HCF behavior of glass fiber-reinforced epoxy composites was developed. It is based on the Wöhler curve analytical expression and the Monte Carlo simulation assessment. By taking into account the variation of the loading parameters (stress and number of cycles), probabilistic Wöhler curves were plotted to predict the high cycle fatigue behavior of the material. In this regard, four cases were studied by varying the hypothesis for the studied stress and number of cycle parameters to be probabilistic or deterministic.

The main results show that, for an applied number of cycles less than 10^7, the reliability is better when the stress or the number of cycle value is probabilistic. Whereas, if the applied number of cycles is more than 10^7, the reliability is better for deterministic values of both stress and number of cycles.

The influence of the composite material parameters (Young's modulus and fiber volume fraction) was also discussed. At this stage, two cases were studied and compared: the first is fibers provided from several suppliers and the second is fibers provided from only one supplier. For both cases, it was found that the variation of glass fibers Young's modulus induces a dispersed Wöhler curve. And by decreasing those Young's modulus values, the composite withstands less loading. Furthermore, it is worth noting that the decrease of the fiber volume fraction induces a decrease of the applied stress and the Wöhler curve becomes more dispersed.

The probabilistic Wöhler curves plotted for various reliability values (1, 25, 50, 75, and 99%) show that, for a given value of applied stress, the reliability and the number of cycles to failure are inversely related. Besides, by taking into consideration the dispersion of fiber volume fraction, we have to decrease the applied stress value to reach the same reliability level. When both material parameters are dispersed (Young's modulus and fiber volume fraction), the probabilistic Wöhler curves exhibit high reliability level for a limited number of cycles to rupture.

The DoE techniques are used in this work by varying the factors of interest in a full factorial design to assess the effect and the interaction of some factors influencing the fatigue reliability.

The controlled input factors of the process are the materials' parameters represented by the variation of fiber and matrix Young's moduli (E_f and E_m) and the fiber volume fraction (V_f), and the loading parameters represented by the applied stress and number of cycles.

Analysis of effects shows that the factors of stress, V_f, E_f, and N, have considerable effect on the reliability, whereas the factor E_m has a negligible effect. The most significant factor on the reliability is observed for the stress variation. When this latter reaches minimum value, the reliability has a maximum value exceeding 80%, and for the highest stress value, the reliability decreases until 0%.

References

1. Caprino G, Giorleo G (1999) Fatigue lifetime of glass fabric/epoxy composites. Compos Part A 30:299–304
2. Nassar MMA, Arunachalam R, Alzebdeh KI (2017) Machinability of natural fiber reinforced composites: a review. Int J Adv Manuf Technol 88:2985. doi:10.1007/s00170-016-9010-9
3. Degrieck J, Van Paepegem W (2001) Fatigue damage modeling of fibre-reinforced composite materials: review. Appl Mech Rev 54: 279–299
4. Wicaksono S, Chai GB (2012) A review of advances in fatigue and life prediction of fiber-reinforced composites. Proc Inst Mech Eng Part L J Mater Des Appl 227(3):179–195. doi:10.1177/1464420712458201
5. Mejri M, Toubal L, Cuillière JC, François V (2017) Fatigue life and residual strength of a short-natural-fiber-reinforced plastic vs Nylon. Compos Part B 110(1):429–441
6. Dadej K, Bieniaś J, Surowska B (2017) Residual fatigue life of carbon fibre aluminium laminates. Int J Fatigue 100(1):94–104
7. Kim J-S, Bae K-D, Lee C, Kim Y-J, Kim W-S, Kim I-J (2017) Fatigue life evaluation of composite material sleeve using a residual stiffness model. Int J Fatigue. doi:10.1016/j.ijfatigue.2017.02.026
8. Mao H, Mahadevan S (2002) Fatigue damage modelling of composite materials. Compos Struct 58(4):405–410
9. Tang HC, Nguyen T, Chuang T, Chin J, Lesko J, Felix WH (2000) Fatigue model for fiber-reinforced polymeric composites. J Mater Civ Eng 12(2):97–104
10. Fish J, Yu Q (2002) Computational mechanics of fatigue and life predictions for composite materials and structures. Comput Methods Appl Mech Eng 191:4827–4849
11. Passipoularidis VA, Philippidis TP, Brondste P (2011) Fatigue life prediction in composites using progressive damage modelling under block and spectrum loading. Int J Fatigue 33(2):132–144
12. Vassilopoulos A.P. (2010) Novel computational methods for fatigue life modeling of composite materials. In: Fatigue life prediction of composites and composites structures (part I: fatigue life modelling). A volume in Woodhead Publishing Series in Composites Science and Engineering. ISBN: 978-1-84569-525-5. pp 139–173
13. Kaminski M.M. (2005) Fracture and fatigue models for composites. In: Computational Mechanics of Composite Materials, Part of the series engineering materials and processes. ISSN 1619-0181 Online ISBN 978-1-84628-049-8 Springer, London, pp 222–295. doi:10.1007/1-84628-049-4_5
14. Bi ZM, Mueller DW (2016) Finite element analysis for diagnosis of fatigue failure of composite materials in product development. Int J Adv Manuf Technol 87:2245. doi:10.1007/s00170-016-8619-z
15. Vassilopoulos A. P & Keller T. (2011) Modeling the fatigue behavior of fiber-reinforced composite materials under constant amplitude loading. In: Fatigue of fiber-reinforced composites, part of the series engineering materials and processes. ISSN 1619-0181 Online ISBN 978-1-84996-181-3 Springer, London, pp 87–139. doi:10.1007/978-1-84996-181-3_4
16. Khoroshun LP, Shikula EN (2012) Deformation and damage of composite materials of stochastic structure: physically nonlinear problems (review). Int Appl Mech 48:359. doi:10.1007/s10778-012-0527-9
17. Jen MHR, Lee CH (1998) Strength and life in thermoplastic composite laminates under static and fatigue loads. Part I: experimental. Int J Fatigue 20:605–615
18. Jen MHR, Lee CH (1998) Strength and life in thermoplastic composite laminates under static and fatigue loads. Part II: formulation. Int J Fatigue 20:617–629
19. Philippidis TP, Vassilopoulos AP (1999) Fatigue strength prediction under multiaxial stress. J Compos Mater 33:1578–1599
20. Liu, Y., & Mahadevan, S. (2010). Probabilistic fatigue life prediction of composite materials. In: Fatigue life prediction of composites and composite structures (pp. 220–248). Elsevier Inc. doi:10.1533/9781845699796.2.220
21. Kawai M, Yano K (2016) Probabilistic anisomorphic constant fatigue life diagram approach for prediction of P–S–N curves for woven carbon/epoxy laminates at any stress ratio. Compos A Appl Sci Manuf 80:244–258
22. Paramonov YM, Kleinhof MA, Paramonova AY (2002) A probabilistic model of the fatigue life of composite materials for fatigue-curve approximations. Mech Compos Mater 38:485. doi:10.1023/A:1021718407399
23. Sokolkin YV, Postnykh AM, Chekalkin AA (1992) Probabilistic model of the strength, crack resistance, and fatigue life of a unidirectionally reinforced fibrous composite. Mech Compos Mater 28: 133. doi:10.1007/BF00613319
24. Chamis CC, Shiao MC (1994) Probabilistic assessment of composite and smart composite structures. In: Spanos PD, Wu YT (eds) Probabilistic structural mechanics: advances in structural reliability methods. International Union of Theoretical and Applied Mechanics. Springer, Berlin
25. Spanos PD, Rowatt JD (1994) A probabilistic model for the accumulation of fatigue damage in composite laminates. In: Spanos PD, Wu YT (eds) Probabilistic structural mechanics: advances in structural reliability methods. International Union of Theoretical and Applied Mechanics. Springer, Berlin
26. Krejsa M, Kala Z, Seit S (2012) Inspection based probabilistic modeling of fatigue crack progression. Procedia Eng 142:146–153
27. Ben SR, Bouraoui C, Fathallah R et al (2007) Probabilistic high cycle fatigue behaviour prediction based on global approach criteria. Int J Fatigue 29:209–221
28. Xiong J. J. , Sheno R. A. (2011) Reliability prediction for fatigue damage and residual life in composites. In: Fatigue and fracture reliability, part of the series Springer Series in Reliability Engineering. ISSN 1614-7839 Online ISBN 978-0-85729-217-9 Springer, London, pp 157–190. doi:10.1007/978-0-85729-218-6_6
29. Cederbaum G., Aboud J. (1991) Reliability of composites based on micromechanically predicted strength and fatigue criteria. In: Composite structures. Online ISBN 978-94-011-3662-4 Springer, Netherlands, pp 75–88. doi:10.1007/978-94-011-3662-4_6
30. Bahloul A, Ben Ahmed A, Mhala MM et al (2016) Probabilistic approach for predicting fatigue life improvement of cracked structure repaired by high interference fit bushing. Int J Adv Manuf Technol. doi:10.1007/s00170-016-9957-6
31. Morel F, Flacelière L (2005) Data scatter in multiaxial fatigue: from the infinite to the finite fatigue life regime. Int J Fatigue 27(9): 1089–1101
32. Hu W, Choi KK, Cho H (2016) Reliability-based design optimization of wind turbine blades for fatigue life under dynamic wind load uncertainty. Struct Multidiscip Optim 54:953. doi:10.1007/s00158-016-1462-x
33. Sakai T, Sakai T, Okada K, Furuichi M, Nishikawa I, Sugeta A (2006) Statistical fatigue properties of SCM435 steel in ultra-long-life regime based on JSMS database on fatigue strength of metallic materials. Int J Fatigue 28(11):1486–1492
34. Jha SK, Chandran KSR (2003) An unusual fatigue phenomenon: duality of the S-N fatigue curve in the β-titanium alloy Ti-10V-2Fe-3Al. Scr Mater 48(8):1207–1212. doi:10.1016/S1359-6462(02)00565-1
35. Lemaire M., Chateauneuf A. & Mitteau J.C. (2005) Fiabilité des structures: couplage mécano-fiabiliste statique, Edit. Hermes Paris, Cote: Rez-de-chaussée: 620.004 52 LEM. [In French]
36. Zhao YG, Ono T (2001) Moment methods for structural reliability. Struct Saf 23:47–75
37. Ditlevsen O, Madsen HO (1996) Structural reliability methods. John Wiley & Sons Ltd, Chichester ISBN 0 471 96086 1

38. Bjerager P (1990) On computation methods for structural reliability analysis. Struct Saf 9:79–96
39. Adimi M.R. (1992) Fatigue loading of pultruded unidirectional composite materials. Comportement en fatigue de materiaux composites unidirectionnels pultrudes. [In French] MScA., Ecole Polytechnique Montreal - Canada, 1992. AADMM86425 MA32(5)1457
40. Adimi, M.R. (1999). Fatigue behaviour of Aramid, carbon and glass FRP rods embedded in concrete. PhD thesis, Dept. of Civil Engineering, Sherbrooke University, Sherbrooke, Quebec, Canada
41. Adimi MR, Rahman H, Benmokrane B (2000) New method for testing fiber-reinforced polymer rods under fatigue. J Compos Constr 4(4):206–213. doi:10.1061/(ASCE)1090-0268(2000)4:4(206)
42. Qiao P, Yang M (2006) Fatigue life prediction of pultruded E-glass/polyurethane composites. J Compos Mater 40(9):815–837. doi:10.1177/0021998305055549
43. Gupta A., Singh H., Walia R.S. (2014) Effect of glass fiber and filler volume fraction variation on mechanical properties of GFRP composite. In: Khangura S., Singh P., Singh H., Brar G. (eds) Proceedings of the International Conference on Research and Innovations in Mechanical Engineering. Lecture Notes in Mechanical Engineering. Springer, New Delhi. doi:10.1007/978-81-322-1859-3_38